

# Antiproton Physics with $\bar{\text{P}}\text{ANDA}$ at FAIR

E. Tomasi-Gustafsson \*

*CEA, IRFU, SPhN , 91191 Gif-sur-Yvette Cedex, France*

*and*

*CNRS/IN2P3, Institut de Physique Nucléaire, UMR 8608, 91406 Orsay, France*

on behalf of the  $\bar{\text{P}}\text{ANDA}$  Collaboration

## Abstract

A high intensity antiproton beam of momenta up to 15 GeV/c will be available at the Facility for Antiproton and Ion Research (FAIR) in the next future. The  $\bar{\text{P}}\text{ANDA}$  experiment is integrated in the storage ring for antiprotons and represents the main pillar of the hadron physics program at this facility. It includes topics like hadron spectroscopy in the charmonium mass region, hyperon physics and electromagnetic processes. This contribution describes the facility FAIR, the detector and the relevant physics issues, with special focus on electromagnetic proton form factors in the time-like region.

## 1 Introduction

The international facility FAIR (Facility for Antiproton and Ion Research) is under construction on the site of GSI (Darmstadt), where the existing structure will be extended and the existing accelerators will serve as injectors and pre-accelerators. It will gather more than 3000 scientists from 50 countries, to study fundamental problems in physics research and applications [1].

The facility will provide a variety of ion beams from proton to uranium of unprecedented quality and intensity, which will be accelerated and delivered to the different areas, allowing to carry out the corresponding programs simultaneously. In the final construction, FAIR will consist of eight ring with up to 1.1 km in circumference, two linear accelerators and about 3.5 km of beam control tubes. High intensity proton beams of intensity up to  $3 \times 10^{13}$  and energy up to 30 GeV will be used directly for different physics programs and to produce secondary beams, such as antiprotons of momenta in the range 1.5-15 GeV/c. The storage and cooler rings will also allow to produce radioactive beams in the energy range 1.5-2 GeV/u, whereas the intensity will be a factor  $10^4$  higher than previously available.

Four main collaborations have been formed, addressing issues in different fields of research. The CBM (Compressed Baryonic Matter) collaboration will focus on proton-proton and proton-nuclei collisions in order to explore a part of the phase diagram of nuclear matter at larger density and lower temperature as compared to high energy experiments as RHIC or ALICE.

The NUSTAR (Nuclear Structure, Astrophysics and Nuclear Reaction) collaboration will study the frontiers of the nuclear stability and the properties of nuclear binding with stable and exotic beams.

The APPA collaboration is a multi-task collaboration, covering several experiments on atomic and plasma physics, biomedicine and material science. Let us quote few examples:

- quantum electrodynamics can be tested in extreme conditions: very high electromagnetic fields can be created by stripping the electrons from heavy ions, which will result in highly charged ions, interacting with antiprotons

---

\*e-mail: etomasi@cea.fr

- the effects of radiation on biological cells is of interest for medicine, radiotherapy and space missions.
- the interaction of very slow antiprotons with atoms and molecules will be studied.
- antiprotons combined with positrons may create anti-hydrogen, which can be used to test fundamental symmetries of the forces governing the nature.

We focus here on the hadron physics experiment with antiproton beams,  $\overline{\text{P}}\text{ANDA}$  [2], which will address different aspects of non-perturbative QCD. The kinematical region accessible at  $\overline{\text{P}}\text{ANDA}$  is relevant for understanding the quark confinement, the origin of the nucleon mass and the creation of charm and strangeness [3].

## 2 The accelerator complex

A scheme of the FAIR complex, the accelerators and the experiment site is shown in Fig. 1. Technological challenges in accelerator physics are faced, as for example the ultra-high vacuum ( $10^{-12}$  mbar) needed to keep recirculating the intense ion beams without losses, or diagnostic systems for very intense beams.

The accelerator will be fed by light and heavy ions high intensity sources. An ECR (electron cyclotron resonance) source will provide 70 mA proton beam current for multi-turn injection into the SIS18 ring. A new proton linear accelerator,  $p$  – *linac*, will be built as an injector for high intensity proton beams. The existing linac UNILAC and ring SIS18 will pre-accelerate the ions before injection to the synchrotron (SIS100) and later, also to a second one (SIS300). Ions will be generated and can further be converted into secondary beams.

Collector, storage and cooling rings will prepare and optimize the properties of the beams for the specific experiments. The operation of the different rings will be coordinated in such a way that up to four experiments can operate simultaneously in the best conditions.

Let us follow the preparation of the antiproton beam: the high intensity proton beam, accelerated by the  $p$  – *linac* to 50 MeV, will be injected in the synchrotrons SIS18/SIS100 and hit the antiproton production target. There,  $10^7$   $p/s$  will be produced at an energy of 3 GeV, and be injected first in the Collector Ring (CR), and then in the High-Energy Storage Ring (HESR).

The high quality of the antiproton beams will be achieved by two kinds of cooling: electron and stochastic cooling. In the CR secondary ion beams and antiprotons undergo stochastic cooling. Antiprotons are then accumulated in the Recycled Experimental Storage Ring (RESR), in order to increase the intensity and cooled using electron and stochastic cooling. In the HESR, the antiproton beams are decelerated down to a momentum of 1.7 GeV/c, or accelerated up to 14.5 GeV/c.

The HESR can have two modes of operation. It can be set in the high intensity mode (peak luminosity  $2 \times 10^{32}$   $\text{cm}^{-2} \text{s}^{-1}$  and momentum spread  $\Delta p/p \approx 10^{-4}$ ) or high resolution mode (ten times reduced peak luminosity and momentum spread  $\Delta p/p \approx 10^{-5}$ ). In the initial time of operation, merely the high resolution mode will be available.

## 3 The $\overline{\text{P}}\text{ANDA}$ detector

The antiproton beam will interact with an internal cluster jet target  $4 \times 10^{15}$   $\text{cm}^{-2}$  thick, at the center of the  $\overline{\text{P}}\text{ANDA}$  detector (pellet and solid targets are foreseen also).

Because the antiprotons that do not interact with the target will recirculate in the HESR,  $\overline{\text{P}}\text{ANDA}$  is a fixed target and an internal target experiment. The ring and the detector are built

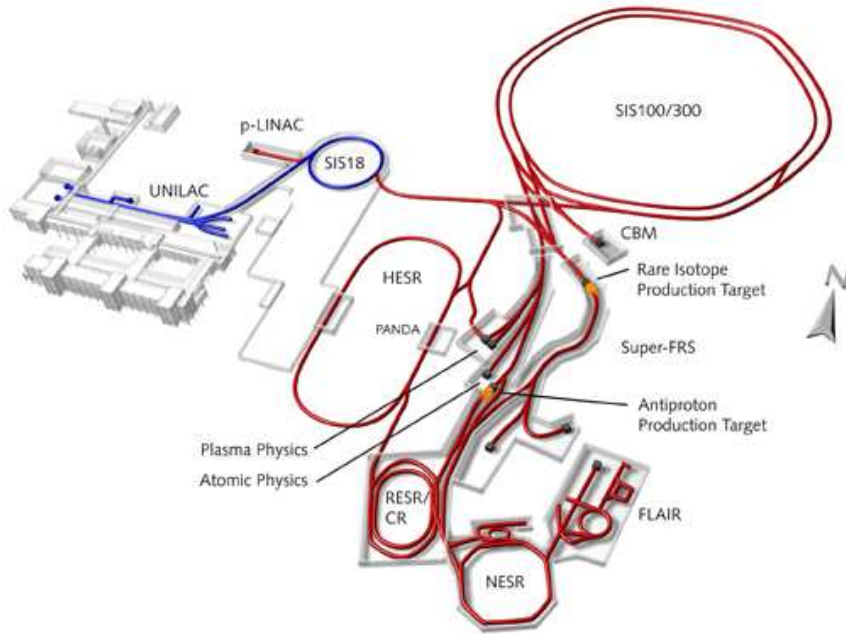


Figure 1: View of the FAIR complex.

and optimized together. Therefore, the performances of this experiment in terms of resolution and luminosity are expected to be better than it was achieved previously.

The detector is a compact assembly of several subdetectors with a flexible design to account for the different physics goals, insuring a close to  $4\pi$  acceptance, excellent tracking capabilities and momentum resolution.

A schematic view of the  $\bar{P}$ ANDA detector is shown in Fig. 2. The size of the detector is about 13 m along the beam direction. It is a compact detector, with two magnets: a central 2T solenoid and a forward dipole magnet. Some of the elements are shortly described below and a detailed description can be found in the dedicated technical design reports [2].

The microvertex detector, with three layers of pixel sensors and two layers of double-sided strips, surrounds the target. The expected resolution is of the order of  $100 \mu\text{m}$ , which is a mandatory requirement for a good vertex reconstruction for  $D$ ,  $K_S$ , and hyperons.

The central tracker consists of straw tubes (STT) to insure a precise spatial reconstruction of the trajectories of charged particles in a broad momentum range from about a few  $100 \text{ MeV}/c$  up to  $8 \text{ GeV}/c$  through the energy loss measurement  $dE/dx$ . The DIRC (Detection of Internally Reflected Cerenkov) will be used for particle identification (PID) at polar angles between  $22^\circ$  and  $140^\circ$ , and momenta up to  $5 \text{ GeV}/c$ . A scintillator tile (SciTil) detector surrounds the DIRC. It will provide fast event timing for a software trigger, relative timing in a multiple track event topology, as well as additional PID in the low momentum region. The foreseen time resolution is of the order of  $100 \text{ ps}$ .

The barrel will be completed by an electromagnetic calorimeter (EM), consisting of Lead-Tungstate ( $\text{PbWO}_4$ ) crystals, to insure an efficient photon detection from  $10 \text{ MeV}$  to  $10 \text{ GeV}$ . The geometry is set to optimize the granularity. The hermeticity of the detection coverage is insured by a forward endcap (3856 crystals) and a backward endcap (600 crystals), in addition to the cylindrical barrel (11360 crystals). A similar type of crystals has been used by the CMS experiment at LHC. However, the specific requirements of  $\bar{P}$ ANDA, such as the photon detection covering a larger energy range as compared to previous experiments, in a high luminosity environment demands new solutions for the detectors, front end electronics and data acquisition. In particular, a low energy threshold at, or below  $3 \text{ MeV}$ , for an individual detector module,

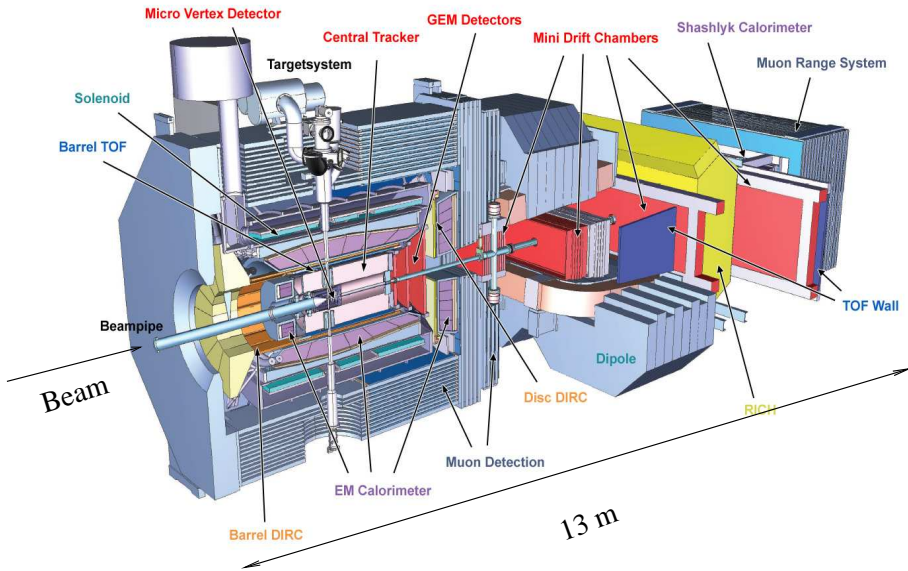


Figure 2: Schematic view of the  $\overline{\text{P}}\text{ANDA}$  detector.

requires the maximization of the  $\text{PbWO}_4$  light yield and the light detection efficiency [4]. An increase of the amount of scintillation light by a factor of four is obtained by cooling the crystals. The  $\overline{\text{P}}\text{ANDA}$  EM calorimeter will be operated at a temperature of  $-25^\circ\text{C}$ . This requires a functional test of all components in a low temperature environment. Moreover, the quality of the crystals themselves has been significantly improved by minimizing the impurities. The light produced by each crystal is read out by two rectangular Large Area Avalanche Photodiodes (LAAPD).

Particles emitted at angles smaller than  $22^\circ$  will be detected by three planar stations of Gas Electron Multiplier (GEM) downstream of the target. The GEM foils can sustain high counting rate due to the high particle flux at forward angles. A hadronic calorimeter is foreseen in the forward region. Aerogel Ring Imaging Cerenkov Counters located in the endcap of the target magnet between polar angles of  $5^\circ$  and  $22^\circ$  will be useful for PID, in particular for  $\pi/K$  separation and information for higher level triggers. The muon identification will be done by Iarocci proportional tubes and with scintillator counters, placed outside and inside the solenoid and dipole magnets, in the inner gap of the solenoid yoke and between the hadron calorimeter planes, with a forward angular coverage up to  $60^\circ$ .

In order to collect different types of events no hardware trigger is foreseen, but continuous data acquisition with fast readout followed by a software event selection is under development.

## 4 The physics program

A scheme of the accessible hadronic channels, of interest for the spectroscopy part of the programme, is shown in Fig. 3. The mass range and the corresponding antiproton momenta are shown on the bottom and top scales, respectively. The light meson sector was previously studied with antiproton beams by LEAR and AGS (for a review, see for instance Ref. [5]). The vertical line shows the upper limit of LEAR. The kinematical region covered by  $\overline{\text{P}}\text{ANDA}$  is especially well suited for charmonium-like and open charm spectroscopy. The high resolution will be crucial for the search and the understanding of the properties of gluonic excitations, as glueball and hybrids.

Models, based on QCD motivated quark potentials containing a Coulomb-like part and

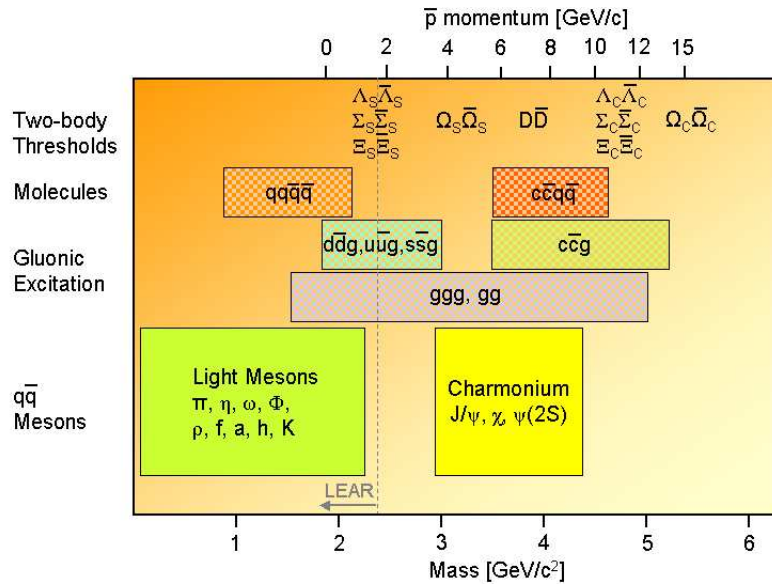


Figure 3: Illustration of the accessible hadronic states. The lower scale shows the mass, the upper scale the corresponding beam momentum where the hadronic states (vertical scale) can be observed.

a confinement term, successfully predict the lower part of the spectrum of charmonium, the bound  $\bar{c}c$  state. The states below the  $D\bar{D}$  threshold are narrow and well separated, therefore they have been well identified by different experiments. Still a better knowledge of some masses and widths, as well as the properties of high angular momentum states, are desirable. Moreover, since a decade, a large number of charmonium-like states have been observed above the  $D\bar{D}$  threshold, that are not predicted by potential models. They are called X, Y, and Z states. Their interpretation is still under debate and their quantum numbers mostly unknown. In particular, the states X(3872) and  $Z_c(3900)$  have been seen by the  $e^+e^-$  facilities working in this energy range, BaBar, BESIII and BELLE, and also seen by CLEO. Observed in different decays, still their nature has not been elucidated: excited charmonium,  $D^0\bar{D}^{*0}$  molecule,  $c\bar{c}g$  hybrid, tetraquarks...[6].  $\bar{P}$ ANDA is expected to bring new important information in this field because of the uniqueness of the antiproton beam at such energy and intensity.

As an example Fig. 4 shows the advantage of the  $\bar{p}p$  annihilations for the determination of the widths of the states of interest. The resonance spectrum of  $\chi_{c1}$  is shown as a function of the center of mass energy in  $\bar{p}p$  annihilation through the reaction  $\bar{p}p \rightarrow \chi_{c1} \rightarrow J\psi\gamma \rightarrow e^+e^-\gamma$  (right scale, green circles) [7]. It is compared to the corresponding spectrum measured with Crystal Ball through  $e^+e^- \rightarrow \psi' \rightarrow \chi_{c1} \rightarrow J\psi\gamma\gamma \rightarrow e^+e^-\gamma\gamma$  (left scale, red circles). The comparison of the obtained resolutions is spectacular. The mass resolution from  $e^+e^-$  is of 10 MeV whereas 240 keV was obtained with antiprotons at FermiLab: in the experiment E835, the formation rate of a resonance is monitored by the beam parameters, and not driven by the energy resolution of the detectors.

As shown by E835 at FermiLab, the resolution which can be achieved with  $\bar{p}$  beams allows a precise energy scan, and the profile of a resonance can be well defined. Note that the resolution expected at  $\bar{P}$ ANDA is expected to improve by a factor of five to ten as compared to previous  $\bar{p}p$  experiments at FermiLab.

$\bar{P}$ ANDA will cover the threshold for charm production, and open the study for open charm associated production. A large sample of  $D_c\bar{D}_c$  pairs will be produced, allowing for studies of CPT violation in the charm sector. The  $D$  meson formed by a light and a heavy quark plays the role of a "QCD hydrogen atom". Heavy charmed meson production at threshold involves

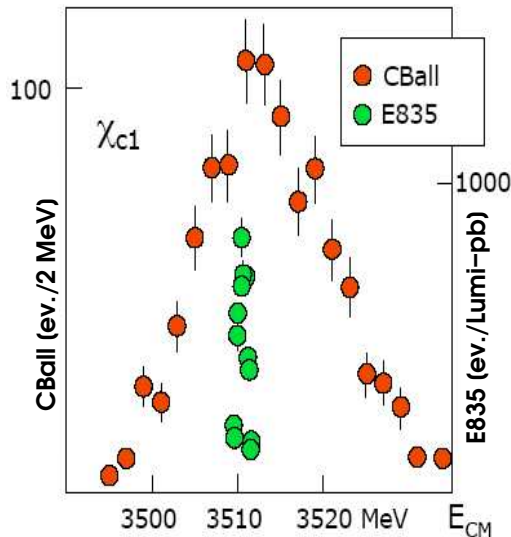


Figure 4: Invariant mass spectrum of  $\chi_{c1}$ , as measured by Crystal Ball (red circles) and E835 (green circles).

on the one hand, a large energy scale, which is necessary to form a  $c$ -quark not pre-existent in the (anti)proton valence quarks, and, on the other hand, low kinetic energies, simplifying the spin structure of the reaction matrix.

It is known that antiproton-proton annihilation creates a gluon-rich environment. The interaction between gluons is attractive. It is believed that the difference between the proton mass and the sum of the masses of the valence quarks is dynamically created by the interacting gluons. New states are expected, with quantum numbers not allowed by the constituent quark model, called "hybrids" ( $q\bar{q}$  pairs with additional gluonic degrees of freedom) or glueballs (meson-like bound state of gluons).

Spectroscopy offers a powerful way to find evidence for gluonic excitations, as shown by the Crystal Barrel at LEAR, and later on by BaBar. The collaboration accumulated a large statistics and detected several resonances, visible in the  $3\pi^0$  Dalitz plot, in particular the  $f_0(1500)$ , discussed to be the lightest glueball candidate, measuring its coupling to its  $\pi\pi$ ,  $\eta\eta$ ,  $\eta\eta'$ , and  $K\bar{K}$  decay channels. The search for a scalar  $J^{PC} = 0^{++}$  (lightest glueball) was done through the reaction  $\bar{p}p \rightarrow \pi^0\pi^0\pi^0$ , where the  $\bar{p}p$  system at rest decays into 3 pseudoscalars. Here, the  $0^+$  resonance decays into two pseudoscalars:  $0^+ \rightarrow 0^-0^-$ , while the third pseudoscalar removes the excess energy [8].

In order to clarify the nature of the observed resonances, the systematic and complete study of the possible decay modes is necessary. Due to the expected high statistics and the possibility of detecting charged and neutral particles as well,  $\bar{P}$ ANDA will bring essential contribution in determining in detail the properties of these states.

Moreover, if a resonance is observed in the data - generally a resonance is accompanied by a light meson- (production mode), subsequently a very precise scan of the corresponding energy region can be performed by tuning the beam energy exactly at the energy where the resonance was seen. If no counting rate excess appears, this is a clear signature of the exotic nature of the resonance. Moreover, if a resonance appears, the measured width will depend on the beam momentum resolution and not on the detector reconstruction, and can thus be measured with excellent precision.

Let us briefly mention hypernuclear physics. Hypernuclei are obtained replacing one (or more)  $u$  or  $d$  quarks by a  $s$  quark. Very few double hypernuclei have been produced and studied up to now. A specific production method with a dedicated set-up will allow to produce

several tens of double hypernuclei/day to be compared to less than 10 (in total) in the past. A unique information on  $\Lambda N$  and  $\Lambda - \Lambda$  interactions which are limited or prevented by the short  $\Lambda$  lifetime in scattering experiments, will be obtained: this represents a unique possibility to study the  $\Lambda - \Lambda$  interaction potential.

A comprehensive review of the topics addressed by  $\overline{\text{P}}\text{ANDA}$  can be found in Ref. [9].

## 5 Time-like electromagnetic proton form factors

Electromagnetic proton form factors (FFs) are fundamental quantities, which contain the dynamical information on the internal charge and magnetic distributions of the proton. The electric and magnetic FFs,  $G_E$  and  $G_M$ , can be accessed, in the time-like (TL) region. For this aim, a precise measurement of the angular distribution of one of the outgoing leptons in the reaction  $\overline{p}p \rightarrow e^+e^-$ , has to be performed, assuming that the reaction occurs through the exchange of a virtual photon of squared momentum  $q^2$  that decays into a lepton pair. Due to the common vertex  $\gamma^* \rightarrow e^+e^-$ , the time reverse reaction  $e^+e^- \rightarrow p\overline{p}$  provides the same physical information on the proton internal structure. Moreover the process  $e^+e^- \rightarrow \overline{p} + p + \gamma$  (initial state radiation) allows to scan a large region of  $q^2$ . When the photon is hard, the cross section of this process can be factorized in a radiator function (that depends on the energy and the angle of the hard photon) and in the cross section for the process of interest:  $e^+e^- \rightarrow \overline{p}p$ .

FFs are complex functions in the TL region, and their moduli squared enter in the expression for the differential unpolarized cross section of the reaction  $\overline{p}p \rightarrow e^+e^-$ : [10]:

$$\frac{d\sigma}{d\cos\theta} = \frac{\pi\alpha^2}{2\beta q^2} \left[ (1 + \cos^2\theta)|G_M|^2 + \frac{1}{\tau} \sin^2\theta|G_E|^2 \right]; \quad \beta = \sqrt{1 - \frac{4M^2}{q^2}}, \quad (1)$$

where  $\tau = q^2/4M^2$ ,  $\alpha$  is the electromagnetic fine constant,  $\beta$  is the beam velocity in the center of mass system, and  $\theta$  is the lepton emission angle. As in the space-like (SL) region, accessible through elastic electron-proton scattering, no interference appears, and the magnetic term is enhanced by the factor  $\tau$ . Unlike in SL region, the differential cross section gives access to the full information on the proton FFs in a single experimental measurement.

The individual determination of FFs in TL region has not yet been done due to the limitation in the intensity of antiproton beams or the luminosity of  $e^+e^-$  colliders, which did not allow a precise and complete measurement of the angular distribution of the outgoing leptons. The results are often given in terms of an effective FF,  $F_p$ , derived from the total (or integrated) cross section under the assumption  $G_E = G_M = F_p$ :

$$|F_p| = \sqrt{\frac{|G_E|^2 + 2\tau|G_M|^2}{1 + 2\tau}}. \quad (2)$$

At the moment the best data comes from BaBar [11, 12] (see Fig. 5), where the effective FF is divided by the dipole function:  $G_D = [1 - q^2/0.71]^{-2}$ . For a recent review the reader can refer to [13]. The data on  $|F_p|$  show indications of several structures, on the overall decreasing trend for the high  $q^2$  values. The threshold region is particularly intriguing. Several experiments have been performed with increasing precision in the near threshold region. A flat behavior as a function of  $q^2$  is observed near threshold. At threshold it is expected that only the S-wave plays a role, and  $|G_E(4M_p^2)| = |G_M(4M_p^2)|$ . Introducing the experimental value of the cross section, one finds  $G(4M^2) = 1$ , like in the case of a point-like fermion [15].

The important contribution from  $\overline{\text{P}}\text{ANDA}$  will be the first individual measurement of the electric and magnetic FFs, in a wide kinematical range. Note that the models which reproduce qualitatively well the existing data in SL region ( $G_E$  and  $G_M$  for proton and neutron) and  $F_p$  in TL region, may give very different predictions for  $G_E$  and hence for the ratio  $\mathcal{R} = |G_E|/|G_M|$ , as well as for polarization observables in TL region [16].

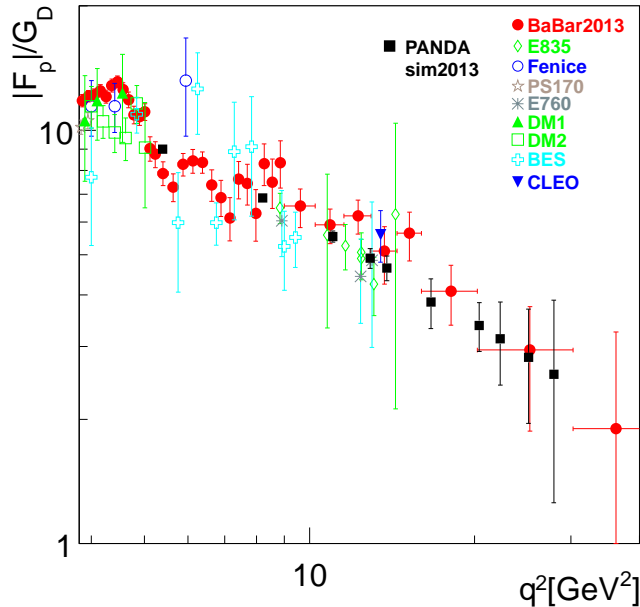


Figure 5: Compilation of the world data on time-like FFs, measured as a function of the momentum transfer squared  $q^2$ . The data from BaBar are shown as red circles (Refs. [11, 12]). The projections for  $\overline{\text{PANDA}}$  are shown as full squares for an integrated luminosity of  $2 \text{ fb}^{-1}$  from Ref. [14].

Experimental attempts for determining  $|G_E|$  and  $|G_M|$  separately, or, more precisely, the ratio  $\mathcal{R}$ , can be found in Ref. [17] (PS170 at LEAR) and more recently in Ref. [11]. The results of the two experiments, although affected by large errors, are not consistent. In the second case a larger value was found in a wide  $q^2$  range above threshold, and a convergence towards unity at large  $q^2$ .

With the luminosity known at a level of a few percent,  $\overline{\text{PANDA}}$  may first determine  $|G_E|$  and  $|G_M|$  separately, for intermediate values of  $q^2$ . The expected uncertainties at  $\overline{\text{PANDA}}$  according to different models are shown in Fig. 6 and they are sufficient to discriminate among the predictions given in the figure.

These data, compared to the corresponding information obtained in electron proton elastic scattering experiments, will constitute a stringent test of the asymptotic behavior predicted by QCD and of analytical properties of the reaction amplitudes. The asymptotic region, where the space-like and time-like values are expected to have the same asymptotic behavior, following analyticity, will be investigated by  $\overline{\text{PANDA}}$ .

Moreover, a detection of a pion accompanying the lepton pair,  $\bar{p}p \rightarrow e^+e^-\pi^0$ , will allow to access for the first time the "unphysical region" below the  $\bar{p}p$  kinematical threshold, following an idea from Ref. [24], updated in Ref. [25].

The main challenge for these measurements is the identification of the lepton pair in a six orders of magnitude larger hadronic background, which consists in particular of two and three pion emission. Simulations show that this is achievable, keeping an efficiency for the signal of the order of 50 % [14].

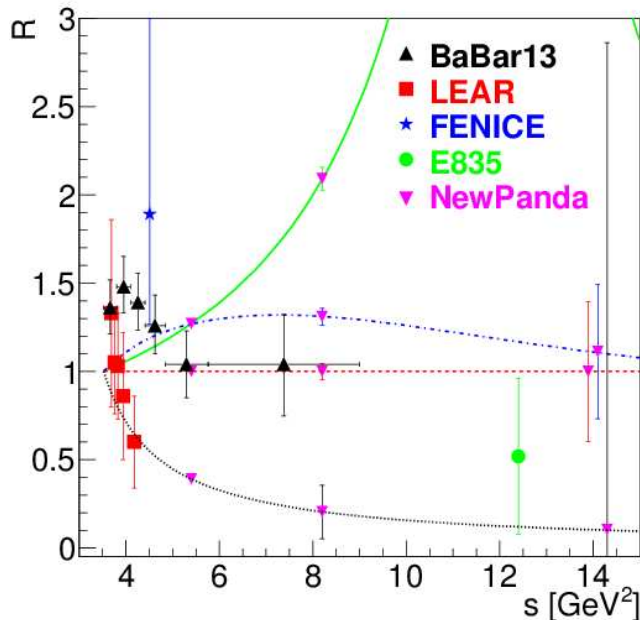


Figure 6: FFs ratio  $\mathcal{R}$  as function of the total energy squared  $s = q^2$ . Data are from: Ref. [11] (black triangles); Ref. [17] (red squares); Ref. [18] (blue star and green circle). The simulated data for  $\overline{\text{P}}\text{ANDA}$  (magenta triangle down) from [14], have been reported along the prediction of different models for the FFs ratio: [19, 20] ( $\mathcal{R} = 1$ , dashed line, red), [21] (solid line, green), [22] (dash-dotted line, blue), [23] (dotted line, black).

## 6 Conclusion

In few years, the FAIR facility will represent the largest European center for nuclear and hadron physics. We have provided a brief overview of the FAIR complex, the  $\overline{\text{P}}\text{ANDA}$  detector and described some items of the physics program in the field of hadron spectroscopy, especially in the charmonium region, search for exotic states, and nucleon structure.

We gave an overview of a part of the foreseen physics program. A review, including also reaction mechanisms, peripheral collisions, in-medium modification of mesons, color transparency, Drell-Yan processes, generalized and transverse parton distributions can be found in the literature [9].

Although many discoveries are ongoing at facilities addressing hadron physics issues, in particular  $e^+e^-$  colliders,  $\overline{\text{P}}\text{ANDA}$  has several advantages. In  $e^+e^-$  collisions only states with the photon quantum numbers  $1^{--}$  can be produced directly in formation mode, whereas states with different quantum numbers can only be observed in the decay of higher resonances. In  $\overline{p}p$  collisions all states with quantum numbers allowed by the selection rules can be directly produced.

The total cross sections for  $\overline{p}p$  annihilation in the  $\overline{\text{P}}\text{ANDA}$  energy domain is of several tens of mb. The cross section for glueball production is expected to be several  $\mu\text{b}$  and the one for hybrids two orders of magnitude lower. Detailed simulations for several reactions and decay channels [3] show the large potential of  $\overline{\text{P}}\text{ANDA}$ . Compared to previous antiproton facilities,  $\overline{\text{P}}\text{ANDA}$  will provide a large improvement in luminosity and beam momentum resolution as well as a better angular coverage and momentum acceptance.

Presently the  $\overline{\text{P}}\text{ANDA}$  Collaboration is formed by 500 researchers from 63 institutions in 18 countries. Technical design reports have been published or are in preparation. A conference, bringing together the FAIR community and discussing the physics program in the light of the

international competition took place recently [26]. The project, which was originally mainly European, is now attracting worldwide collaborators.

## References

- [1] The new large scale accelerator facility in Europe website, URL: <http://www.fair-center.eu>.
- [2] <http://www.gsi.de/PANDA>.
- [3] [The PANDA Collaboration], Physics Performance Report for PANDA. arXiv:0903.3905 [hep-ex];
- [4] M. Kavatsyuk *et al.* [PANDA Collaboration], Nucl. Instrum. Meth. A **648** (2011) 77.
- [5] C. B. Dover, T. Gutsche, M. Maruyama and A. Faessler, Prog. Part. Nucl. Phys. **29**, 87 (1992).
- [6] N. Brambilla, *et al.*, Eur. Phys. J. C **74** 2981 (2014) 10.
- [7] M. Andreotti *et al.*, Nucl. Phys. B **717** (2005) 34.
- [8] C. Amsler *et al.*, [Crystal Barrel Collaboration], Phys. Lett. B **342** (1995) 433.
- [9] U. Wiedner, Prog. Part. Nucl. Phys. **66** (2011) 477.
- [10] A. Zichichi, S. Berman, N. Cabibbo, R. Gatto, Nuovo Cim. **24** (1962) 170.
- [11] J. Lees, *et al.*, Phys. Rev. D **87** (2013) 092005.
- [12] J. P. Lees *et al.* [BaBar Collaboration], Phys. Rev. D **88** (2013) 072009.
- [13] S. Pacetti, R. Baldini-Ferroli and E. Tomasi-Gustafsson (2014), DOI: 10.1016/j.physrep.2014.09.005.
- [14] A. Dbeyssi, Ph.D. thesis, Université Paris-sud (2013).
- [15] R. Baldini, S. Pacetti, A. Zallo, A. Zichichi, Eur. Phys. J. A **39** (2009) 315.
- [16] E. Tomasi-Gustafsson, F. Lacroix, C. Duterte, G. Gakh, Eur. Phys. J. A **24** (2005) 419.
- [17] G. Bardin, *et al.*, Nucl. Phys. B **411** (1994) 3.
- [18] R. Baldini, *et al.*, Eur. Phys. J. **C46** (2006) 421.
- [19] V. Matveev, R. Muradyan, A. Tavkhelidze, Teor. Mat. Fiz. **15** (1973) 332.
- [20] S. J. Brodsky, G. R. Farrar, Phys. Rev. Lett. **31** (1973) 1153.
- [21] F. Iachello, Q. Wan, Phys. Rev. C **69** (2004) 055204.
- [22] E. L. Lomon, S. Pacetti, Phys. Rev. D **85** (2012) 113004.
- [23] E. Kuraev, E. Tomasi-Gustafsson, A. Dbeyssi, Phys. Lett. B **712** (2012) 240.
- [24] M. P. Rekalov, Sov. J. Nucl. Phys. **1** (1965) 760.
- [25] E. A. Kuraev, *et al.*, J. Exp. Theor. Phys. **115** (2012) 93.
- [26] International conference on Science and Technology for FAIR in Europe 2014, Worms, October 13-17, 2014, <http://indico.gsi.de/conferenceDisplay.py?confId=2443>.